Journal of The Electrochemical Society, **152** (5) A882-A891 (2005)
0013-4651/2005/152(5)/A882/10/$7.00 © The Electrochemical Society, Inc.

Transport Properties of $LiPF_6$-Based Li-Ion Battery Electrolytes

Lars Ole Valøen[a,*,z] and Jan N. Reimers[a]

[a]*E-One Moli Energy (Canada), Limited, Maple Ridge, British Columbia V2X 9E7, Canada*

The electrolyte plays an important role in governing the high-current performance of Li-ion batteries. Normally, battery electrolytes are optimized for maximum conductivity. In order to gain a more profound understanding of the role of the electrolyte, properties such as the Li salt diffusion coefficient, the Li^+ transference number, and the Li salt activity all need to be measured in addition to the conductivity. The situation is further complicated by the fact that high currents change the cell temperature and also create strong concentration gradients in the electrolyte. A full set of transport properties for $LiPF_6$ in a propylene carbonate/ethylene carbonate/dimethyl/carbonate mixture were measured as a function of temperature and $LiPF_6$ concentration. The Li^+ transference number was found to be fairly constant with concentration. The activity and diffusion coefficient were both found to vary strongly with temperature and concentration. The temperature dependence of the transport properties is shown to be crucial for making predictions of cell performance at high currents.
 [DOI: 10.1149/1.1872737]

Manuscript submitted August 4, 2004; revised manuscript received September 16, 2004. Available electronically March 30, 2005.

The commercial viability of Li-ion cells in the portable electronics marketplace is now well established. These cells are optimized for maximum volumetric energy density, often at the expense of rate capability. The low conductivity of the nonaqueous liquid electrolytes used in these cells, when compared to the relatively high conductivity of aqueous electrolytes, has led to the common misconception among Li-ion users that Li-ion technology is unsuitable for applications which require high currents. To compensate for the low conductivity of the electrolyte, Li-ion cells use rather thin electrode stacks with a thickness around 200-400 μm. Li-ion cells also have about three times the voltage of most aqueous battery chemistries. These, and other effects combined, result in gravimetric and volumetric power densities, in a properly designed Li-ion cell, that can be far in excess of any other commercialized, secondary battery chemistry.

In spite of their high power densities (>1000 W/kg, >2000 W/L[1]), Li-ion cells aimed at high power applications still require further optimizations, more for the purposes of reducing cost ($/kW) than for reduction of pack size. When optimizing for power, one must consider all cell components, but the electrolyte stands out as one component that is easy to modify, and also easy to measure *ex situ* (*i.e.*, in a beaker on the lab bench). Typically the density, viscosity, freezing point, and most notably the conductivity are measured when characterizing electrolytes. In the literature, work focused on conductivity measurements is readily available.[2-10] In order to predict, or at least speculate about cell performance, one must measure conductivity as a function of temperature and electrolyte salt concentration. The temperature dependence is important because in general, a Li-ion cell will self heat during medium- or high-current operation, thus improving its rate capability as the discharge (or charge) proceeds. The concentration dependence is important because gradients in the salt concentration usually develop during high-current discharge (or charge). However, full knowledge of the conductivity does not allow for estimation of the magnitude of these concentration gradients, or even the voltage polarization that results from a concentration gradient, because the conductivity only tells us the voltage drop over a specified electrolyte thickness in absence of concentration gradients.

In principle the number of independent phenomenological transport parameters for a mixture of n different species is, according to the Onsager reciprocal relations, given by $n(n-1)/2$.[11] In order to simultaneously optimize the viscosity and dielectric constant, all commercial Li-ion cells use 2 or more solvent species. For example, a system with $LiPF_6$ in propylene carbonate/ethylene carbonate/dimethyl carbonate (PC/EC/DMC), is in principle described by ten independent transport properties. This is almost guaranteed to discourage anyone from attempting to fully characterize a commercial electrolyte. However, if the solvent mixture is treated as one component, the number of independent transport properties drops to a more manageable three, and according to Ref 12, this does not appear to introduce significant error for realistic battery electrode conditions. In this case any differences in the interactions between Li^+ and each solvent species are ignored.[13] As a practical matter it makes sense to at least begin by ignoring these effects, and treat the solvent as one species. For the moment it is conventional to refer to the three-parameter characterization, as full characterization. In addition to the $n(n-1)/2$ transport properties one must also measure the salt activity in order to predict voltage polarization in the presence of concentration gradients. For simplicity we loosely refer to activity as a transport property, although it is a thermodynamic property.

Therefore in order to fully characterize a Li-ion electrolyte one should at least measure the following properties as a function of concentration and temperature: (*i*) the conductivity, usually denoted as $\kappa(c,T)$; (*ii*) the salt diffusion coefficient, usually denoted as $D(c,T)$; (*iii*) the cation (or anion) transference number (often referred to as the transport number), usually denoted as $t_+(c,T)$; and (*iv*) the salt activity, often characterized as the mean molar activity coefficient, $f_\pm(c,T)$.

It is D and t_+ which determine the concentration gradients that form under load, and $f_\pm$ which determines any voltage polarization resulting from the gradient. For understanding high-current effects, none of these latter three can be ignored. In practice only some of these properties are strongly temperature dependent in the range of interest, $-30 \rightarrow \sim 60$°C. It is often assumed that we only need data in a narrow concentration range near 1.0 M, because that is the starting concentration in many commercial Li-ion cells, as well as cells studied in the literature. As Doyle and Fuentes[14] have already pointed out, modeling concentration gradients for discharge currents as low as 2 C yields concentrations in excess of 2 M for the anode. Higher currents would further increase this concentration. So measured transport properties in the concentration range from infinite dilution up to the saturation limit are relevant and useful.

Examples in the literature of D and t_+ measurements are rare[4,5,15-19] and usually not as functions of concentration or temperature. The literature surrounding salt activity for liquid Li-ion electrolytes is almost nonexistent, except for the innovative work by Georen and Lindbergh,[20] characterizing various transport properties in lithium battery gel electrolytes using the $LiClO_4$ in PC system. The reason for the limited availability of literature data is assumed to be twofold, (*i*) for understanding energy-optimized cells, which are only expected to run low currents, knowing the conductivity is

* Electrochemical Society Active Member.
z E-mail: larsv@molienergy.com

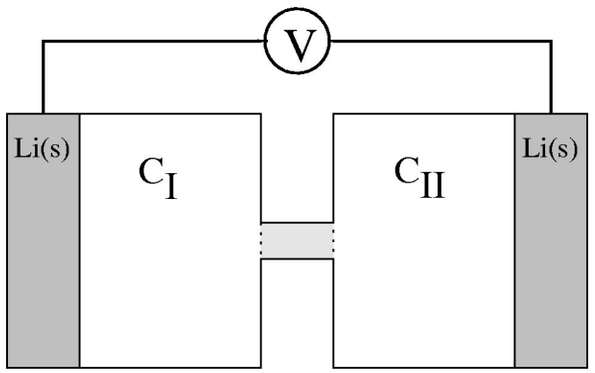

Figure 1. Concentration cell. The shaded middle area of the cell prevents mixing of the two electrolytes of concentrations C_I and C_{II}.

believed to be sufficient, and (*ii*) conductivity measurements are trivial, using turn key equipment, and measurements of the other three properties are most certainly not trivial.

At this point we must acknowledge the innovative work done by the Berkeley group[21-24] in their measurements of a complete set of transport properties for a polymer electrolyte system. They began by studying $PEO_nNa^+CF_3SO_3^-$ using concentration cells of the form $Na|PEO_nNaCF_3SO_3|PEO_mNaCF_3SO_3|Na$ and using the well-known differential relationship between concentration, c, and cell potential, Φ

$$d\Phi = \frac{2RT}{F}(1 - t_+)d\ \ln(f_\pm c) = \frac{2RT}{F}(1 - t_+)\left(1 + \frac{d\ \ln f_\pm}{d\ \ln c}\right)d\ \ln c \qquad [1]$$

where the mean molar activity coefficient, $f_\pm$ has been isolated from the concentration in the right side. Strictly speaking, in the logarithm we should write $\ln c/c_o$, but the reader should keep in mind that we are differentiating so $d\ \ln c/c_o = d\ \ln c$ exactly. As is often the case with electrolyte property measurements, the concentration cell can measure an algebraic combination of two properties (the transference and activity) but is unable to tell us either property in isolation. Ma *et al.*[21] then used a galvanostatic polarization technique to determine the transference and diffusion coefficient. While the concentration cell method is generally applicable to both polymer and liquid electrolyte systems, the other techniques used by Ma *et al.*[21] are best suited to polymer systems. As discussed in detail later, for Li^+-liquid systems we must take care to minimize both convection effects and Li-dendrite effects. As compensation for these difficulties, with liquid systems the age-old Hittorf method[25] can be applied for measuring the transference number.

Concentration potential.—Technique.—In order to compare with a real Li (left) $|Li^+PF_6^-||Li^+PF_6^-|$ Li (right) concentration cell as shown in Fig. 1, we must integrate Eq. 1 into finite difference form. This must be done with care because in general both t_+ and $f_\pm$ are concentration dependent and therefore vary across the width of the concentration cell. We begin by writing Eq. 1 in a more convenient form

$$d\Phi\frac{F}{2RT} = v(c,T)d\ \ln c \qquad [2]$$

where all the unknowns are contained in the function $v(c,T)$

$$v(c,T) = (1 - t_+)\left(1 + \frac{d\ \ln f_\pm}{d\ \ln c}\right) \qquad [3]$$

There is no general theory for the behavior of the transference at low concentrations other than it is expected to be constant, but Debye-Hückel theory does predict the behavior of the activity as $c \to 0$

$$\frac{\partial\ \ln f_\pm}{\partial\ \ln c} \approx -A\frac{1}{2}c^{1/2} + \text{ constant}(c)$$

The constant A can be evaluated if the dielectric constant for the solvent is known.[25] This together with the Taylor expansion for $f_\pm$ given by Newman[11] suggests that a Taylor expansion for $v(c,T)$ would efficiently (*i.e.*, without too many terms) represent the true behavior

$$v(c,T) = v_0(T) + v_1(T)c^{1/2} + v_2(T)c^1\cdots = \sum_{i=0}^{n} v_i(T)c^{i/2} \qquad [4]$$

which can be integrated term by term in order to obtain a finite difference version of Eq. 1. Hence

$$\int_L^R d\Phi\frac{F}{2RT} = \frac{\Delta\Phi F}{2RT} = v_0(T)[\ln c]_{c_L}^{c_R} + \sum_{i=1}^{n} v_i(T)\frac{2}{i}\left[c^{i/2}\right]_{c_L}^{c_R}$$
$$= v_0(T)[\ln c_R - \ln c_L] + 2v_1(T)[\sqrt{c_R} - \sqrt{c_L}]\cdots$$
$$+ v_2(T)[c_R - c_L] + v_3(T)\frac{2}{3}\left[c_R^{\frac{3}{2}} - c_L^{\frac{3}{2}}\right]\cdots \qquad [5]$$

where c_L and c_R are, respectively, the salt concentrations on the left and right side of the cell. (For convenience in notation we have absorbed factors of $(1/c_o)^{i/2}$ in the v_i expansion coefficients.) Note that because of the assumed nonlinear behavior of $v(c,T)$, the cell potential is a function of the absolute concentrations on both sides of the cell, and not just a function of Δc (or $\Delta \ln c$) as is assumed in most textbooks. The expansion coefficients $v_i(T)$ can easily be determined by linear least-squares fitting to a series of $\{\Delta\Phi(T),c_L,c_R\}$ data triplets. One is free to include as many terms in the expansion as are required to faithfully represent the measured data. In practice we find four terms are sufficient for Li-ion electrolytes. Closed-form expressions for the activity coefficient have been proposed,[11,26] but we had less success describing our data using these.

Once t_+ and $v(c,T)$ are known, the factor $\partial\ \ln f_\pm/\partial\ \ln c$ can be extracted. According to Debye-Hückel theory (Eq. 2) we can assume that $\lim_{c\to 0}\partial f_\pm/\partial c = 0$. If the transference number is assumed to be constant with concentration, the following expression can be obtained for the activity coefficient

$$\ln f_\pm = \frac{1}{1 - t_+}\sum_{i=1}^{n}\frac{2}{i}v_i(T)c^{i/2} \qquad [6]$$

The concentration cell shown in Fig. 1 has a dual purpose. Once the potential as a function of concentration differences is determined, this can be used as a convenient measure for the concentration.

Previous results.—As previously noted, the availability of literature concerning salt activity for Li-ion battery electrolytes is limited. The studies of Georen and Lindbergh[20] predict an increase in the activity with increasing concentration up to 2 M for for $PC/LiClO_4$ assuming a limited variability of the Li^+ transference number and a small variation in activity from infinite dilution up to ~0.1 M.

Transference number.—Technique.—By treating the solvent as one component and assuming small concentration gradients, the Hittorf method can be applied for the determination of transference numbers; a charge is transferred from one electrolyte chamber to another chamber and the change in potential at open circuit is determined. A schematic overview of the processes is given in Fig. 2.

If the $LiPF_6$ diffusion is ignored, the accumulation on the anode side can be expressed as

$$\Delta c_a = \frac{\Delta n}{V_a} = t_-\frac{q}{V_aF} = (1 - t_+)\frac{It}{V_aF} \qquad [7]$$

Here the subscript a refers to the anode chamber, Δc is the concentration change, V is the volume, Δn is the change in the number of atoms in the anode chamber, and t_+ and t_- the transference numbers.

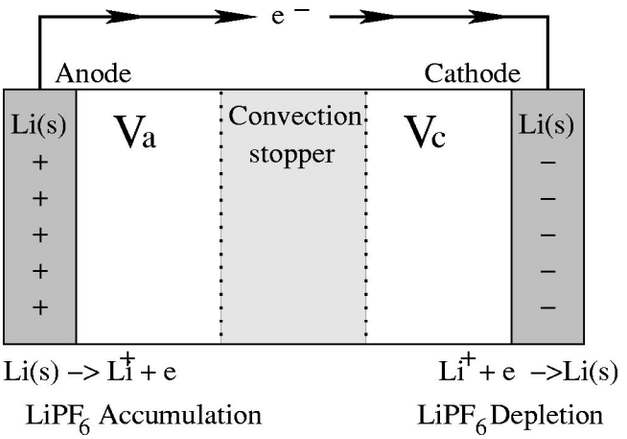

Figure 2. Transference number determination principle. The shaded middle area of the cell prevents mixing of the two electrolytes.

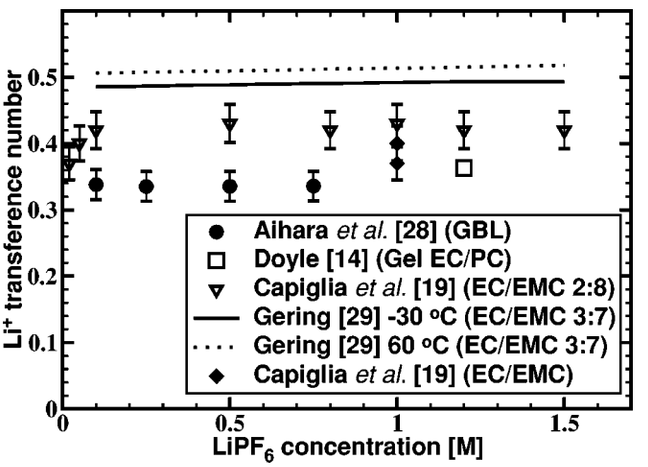

Figure 3. Literature values for the Li^+ transference number in $LiPF_6$ collected for various solvents. Error bars indicate one standard deviation for values obtained using pfg-NMR. Standard deviation calculations are based on information provided by Clericuzio *et al.*[28]

Furthermore, q is the charge, I is the current, and t is the time of the experiment. Similarly the cathode depletion is

$$\Delta c_c = -\frac{\Delta n}{V_c} = -t_+ - \frac{q}{V_c F} = (t_+ - 1)\frac{It}{V_c F} \quad [8]$$

where subscript c refers to the cathode chamber. The total concentration difference is then obtained by combining Eq. 7 and 8

$$\Delta c = \Delta c_a - \Delta c_c = \frac{It(1 - t_+)}{F}\frac{V_c + V_a}{V_c V_a} \quad [9]$$

Rearranged, this gives an expression for the transference number

$$t_+ = 1 - \frac{V_c V_a}{V_c + V_a}\frac{F\Delta c}{It} \quad [10]$$

For small potential differences, we can use Eq. 2 and $v(c,T)$ as determined from the concentration cell to estimate Δc from the cell potential

$$t_+ = 1 - \frac{V_c V_a}{V_c + V_a}\frac{F^2\Delta\Phi}{2ItRT}\frac{c_o}{v(c,T)} \quad [11]$$

where $c_o = c_R + c_L/2$. If $\Delta\Phi$ is large, Eq. 5 must be inverted to obtain an accurate value for Δc; however, such a situation should be avoided as the transference number is only well defined when Δc is small. The transference number can be found from Eq. 11 by applying a fixed current for a known time and monitoring the resulting change in open-circuit potential (OCP).

Previous results.—In spite of the importance of the Li^+ transference number, there is a limited selection of literature data for electrolytes intended for utilization in Li-ion batteries. According to Capiglia *et al.*,[19] the diffusion coefficient for ^{19}F in PF_6^- is higher than the diffusion coefficient for ^7Li, giving $t_{PF_6^-} > t_{Li^+}$. This is presumably because ^7Li needs a larger number of solvent molecules in its solvation shell. Experimental values of $t_+ = 0.37-0.43$ have been reported[19] for concentrations up to 1.5 M of $LiPF_6$ in EC/EMC. The experimental error in the transference number determination was not given but has elsewhere been estimated to be around 5% in binary and 20% in ternary solutions for the method used pulsed field gradient-nuclear magnetic resonance (pfg-NMR).[27] The Li transference number in $LiPF_6$ was furthermore reported to be $t_+ = 0.363$ for a concentration of 1.2 M $LiPF_6$ in lithium polymer cells[14] and around 0.34,[28] independent of concentration for 0.1−0.8 M $LiPF_6$ in γ-butyrolactone (GBL) solvent. Gering and Duong[29] predicted an array of of electrolyte transport properties using a solvation-based chemical physics model, finding a Li^+ transference number close to 0.5 in EC/EMC-$LiPF_6$, slightly increasing with temperature and $LiPF_6$ concentration. In Fig. 3, literature values for the Li^+ transference number in $LiPF_6$ collected for various solvents is given. Error bars indicate one standard deviation for values obtained using pfg-NMR. Standard deviation calculations are based on information provided by Clericuzio *et al.*[27] From Fig. 3, we see that the experimental values for t_+ are similar, regardless of temperature, $LiPF_6$ concentration, and solvent mixture. This indicates that, within certain limits, the transference number behaves almost like an intrinsic property of the dissolved salt. However, we must keep in mind that these measurements do not extend to high concentrations where one might expect incomplete solvation shells to influence the transference number. The data given by Gering and Duong[29] indicate a limited temperature dependence for t_+.

Diffusion coefficient.—*Technique*.—The diffusion coefficient can be determined from the relaxation of a concentration difference in an experimental cell as the one shown in Fig. 4. The concentration gradients can be analyzed for short times (semi-infinite diffusion, galvanostatic polarization method)[30] or for long times (restricted diffusion).[31]

Concentration gradients can be generated *in situ*, or the cell can be made up using two different concentrations for the anode and the cathode. To measure the diffusion coefficient, the concentration gra-

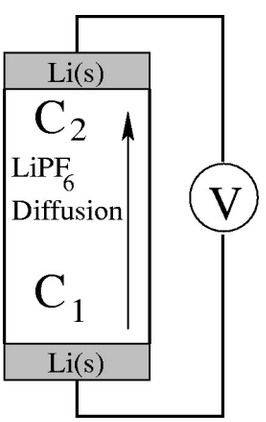

Figure 4. Diffusion coefficient determination principle, diffusion cell. At the start of the experiment, $C_1 = C_2$, after applying a constant current for a predetermined time, $C_1 > C_2$.

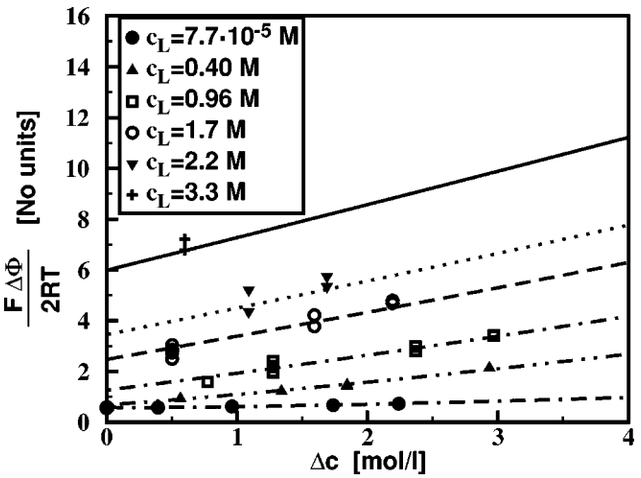

Figure 5. Fit to Eq. 4 for experimental concentration cell data taken at 294 K. $\Delta c = c_R - c_L$ and $c_L < c_R$ where c_L and c_R denote, respectively, the concentration in the left and right chamber of the concentration cell.

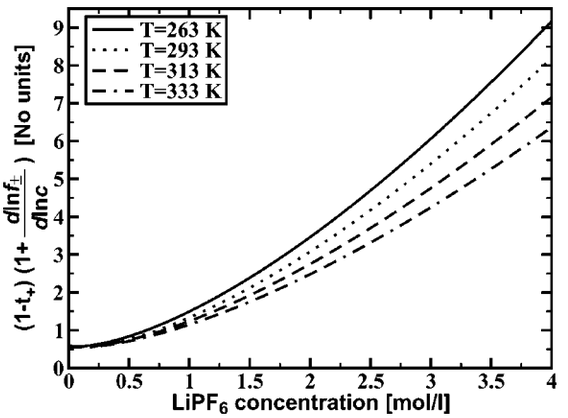

Figure 6. Thermodynamic factor $v(c,T) = (1 - t^+) \cdot (1 + \mathrm{d} \ln f_\pm / \mathrm{d} \ln c)$ as a function of $LiPF_6$ concentration determined from concentration cell data for 263, 293, 313, and 333 K.

dient is allowed to relax and the potential is monitored. The diffusion coefficient is then extracted using the appropriate cell parameters. For the measurements applied in this paper, it was chosen to analyze the short time relaxation because those measurements appeared to be less sensitive to any mechanical vibrations felt by the electrochemical setup and therefore gave more consistent results. The details of the measurements including the intermediate steps are shown in the Results section.

Previous results.—Capiglia *et al.*[19] determined diffusion coefficients for an EC/EMC mixture in the range of 1×10^{-6} to 7×10^{-6}cm^2/s for ^{19}F in PF_6^- and for $^7Li^+$, observing a decreasing trend with increasing concentration up to 1.5 M. For an EC/DEC mixture, diffusion coefficients in the range of 5×10^{-7} to 2×10^{-6}cm^2/s for $^7Li^{+}$[32] were observed.

Experimental

Electrolytes with $LiPF_6$ concentrations from 7.7×10^{-6} to 3.9 M were made by adding $LiPF_6$ salt (Stella, >99.9%) to a mixture of PC (10 vol %), EC (27 vol %), and DMC (63 vol %) (Mitsubishi). All processes involving electrolyte exposure were performed in a moisture-controlled atmosphere (dew point between −35 and −40°C), at a constant temperature of 21°C. All parts to be subjected to electrolyte exposure during measurements were vacuum dried at 70°C prior to exposure. Electrolyte conductivities were measured using a YSI model 35 conductance meter. Concentration potentials at room temperature were measured using a cell with two chambers connected by a stopcock. Both chambers were allowed to equilibrate before the stopcock was opened and the potential determined using a Solartron 1286 electrochemical interface. Concentration potentials at other temperatures were measured in a fully submersible cell with two chambers separated by a Teflon tube using an E-One Moli Energy charger system with a Keithley model 196 system DMM high-impedance-voltage measurement unit coupled to a Keithley 705 scanner. The Teflon tube connector was filled with inert polyethylene beads (General Polymer) to prevent convection. A smaller diameter Teflon tube with one end closed by three layers of a biaxial strength separator (Mitsui) was put in four different locations inside the Teflon tube connector to prevent mixing of the two electrolytes. The entire cell was submerged in a controlled temperature bath for temperatures from −20 to +60°C. The cell potential was measured after stabilization using lithium foil electrodes.

The transference number was obtained from a two-chamber cell. The two chambers were separated by a Teflon tube filled with high- density polyethylene (HDPE), General Polymer, held in place by a biaxial strength separator (Mitsui) to prevent mixing of the two electrolytes. Both ends of the tube were closed to convection by applying a perforated biaxial strength separator (Mitsui). The measurement was initiated using the same electrolyte in both chambers. A stirbar was put in each chamber to ensure homogeneous chamber concentration. A small current was then applied for a predetermined time. The cell was then allowed to rest until the potential stabilized. The rest potential was used to calculate the concentration difference created by the applied current. This procedure was applied for a number of steps to ensure a minimum error in the measurement.

Diffusion coefficients were extracted using the galvanostatic polarization method[30] using the E-One Moli Energy charger system. Custom-designed cylindrical cells of 100 mm length and diameters ranging from 5 to 20 mm were used for the measurements. The cells were filled with the desired electrolyte, Li metal electrodes were put on each end of the cell, and the cell ends were sealed off so that neither electrolyte nor lithium foil were exposed to the atmosphere. The cells were placed vertically inside a controlled temperature chamber, and a small current was applied for a duration of 45-180 min. The current and duration were selected to ensure semi-infinite diffusion conditions. The data was extracted and processed as described by others.[21,30]

Results and Discussion

Concentration potentials.—Because the measurement of transference numbers and diffusion coefficients are strongly reliant on the determination of concentration potentials, great care was taken to provide accurate and reproducible concentration cell results. The quality of the fit characterized by the relative uncertainty of the fit parameters was independent of temperature. In Fig. 5, as an example, the resulting quality of the fit to Eq. 4 with $n = 3$ is given for experimentally measured potential differences at 294 K.

The fit to the experimental data is good, especially for the lower concentrations. The fit presented in Fig. 5 was found to be representative for the fits obtained for different temperatures. As can be seen from Fig. 5, there is a slight tendency to underestimate the voltage drop for a given concentration difference for concentrated solutions. In Fig. 6, the resulting factor $v(c,T) = (1 - t^+) \times (1 + d \ln f_\pm / d \ln c)$ is shown as a function of $LiPF_6$ concentration for different temperatures. The lines were obtained by fitting each temperature independently.

From Fig. 6, a temperature dependence of $v(cT)$ can be observed for high $LiPF_6$ concentrations, but for the low concentrations the determined temperature dependence is within error. This observation

Table I. The parameters and their respective correlation coefficients resulting from fitting the data shown in Fig. 6, forcing linear temperature dependence.

Parameter	Value	σ	σ(%)	$C_{v_{00}}$	$C_{v_{10}}$	$C_{v_{30}}$	$C_{v_{31}}$
v_{00}	0.601	0.003	0.5	100	−83	67	21
v_{01}	0	0	0	-	-	-	-
v_{10}	−0.24	0.01	5.5	−83	100	−88	−27
v_{11}	0	0	0	-	-	-	-
v_{20}	0	0	0	-	-	-	-
v_{21}	0	0	0	-	-	-	-
v_{30}	0.982	0.006	0.6	67	−88	100	23
v_{31}	−0.0052	0.0001	2.4	21	−27	23	100

suggests using linear temperature dependence the for $i = 3$ term, *i.e.*, $v_3(T) = v_{30}[1 + v_{31}(T - T_o)]$, which allows one to simultaneously fit the data for all temperatures. With this simplification the resulting parameters from the fit are given in Table I. Several terms were not significant (*i.e.*, the relative error was high) for the fit and were kept fixed at zero. Most notably the term v_{01} was not needed for the fit, indicating that the temperature dependence of the transference number at low concentrations can be ignored. That we can faithfully fit all concentration cell data for a wide range of concentrations and temperature using only four parameters is a rather elegant result.

Using magnification of the low-concentration part of Fig. 6, it can be furthermore observed that the data for $v(c,T)$ shows a shallow minimum for low concentrations. For moderate and high concentrations, the factor $v(c,T)$ increases with concentration. This type of behavior has previously been observed for other electrolytes such as acetic acid, HCl and HNO_3[11] as well as for a number of alkaline and earth alkaline halides.[25] For the alkaline halides, the minimum was reported to shift toward higher concentrations as the principal quantum number increased.[25] In comparison, for the current system, the minimum in $v(c,T)$ is at a relatively low concentration. The graph shown in Fig. 6 shows that assuming a limited variation in the transference number, the activity coefficient, $f_{\pm}$, may be decreasing slightly with concentration for small $LiPF_6$ concentrations, indicating some ion association. For moderate and high concentrations, the activity coefficient is increasing rapidly with concentration. According to Pletcher,[33] for practical purposes the activity may be thought of as the "effective concentration" of a species. The high activity therefore indicates an effective concentration that is much higher than the molarity of the electrolyte should indicate. The number of salt molecules per liter of solvent is roughly five times higher in water than in the PC/EC/DMC mixture used here, meaning that a 1 M solution could be roughly compared to a 5 M aqueous solution. This explains part of the fact that any minimum in the $v(c,T)$ function occurs at a low concentration, suggesting that $LiPF_6$ in PC/EC/DMC-based electrolytes can be seen as concentrated solutions, even for low concentrations.

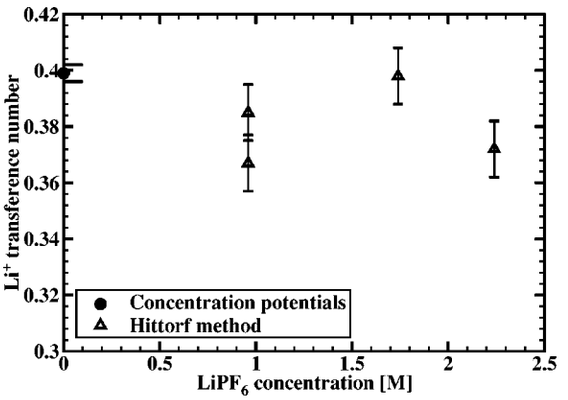

Figure 8. Li^+ transference number as a function of concentration. Error bars are estimated standard deviation.

Li^+ transference number.—From Table I, we see that in the limit $c \to 0$, t_+ can be determined as $(1 - v_{00}) = 0.399 \pm 0.003$. Any temperature dependence of v_{00} was found to be insignificant for the quality of the fit, indicating that temperature dependence of the transference number is negligible at infinite dilution. For finite concentrations we must rely on the less precise Hittorf method.

In Fig. 7, the potential difference as a function of charge transferred in a Hittorf cell for a 1.7 M electrolyte is given. The result is linear and using Eq. 11 and anodic and cathodic volumes of 9.53 and 9.56 mL, respectively, yields $t_+ = 0.398$. In Fig. 8, the Li^+ transference number is given as a function of concentration.

From Fig. 8, one can observe that the noise level of the determination of th Li^+ transference number as a function of concentration is significant when using the Hittorf method. Any concentration dependence in t_+ at 21°C for $LiPF_6$ concentrations in the range from 0.96 to 2.2 M was within the noise limits of the experiment. For further calculations, t_+ is assumed to be 0.38 for all concentrations and temperatures. This value is similar to the values reported in literature and shown in Fig. 3.

Activity coefficient.—With knowledge of t_+ we can now disentangle the concentration cell results to isolate salt activity. In Fig. 9,

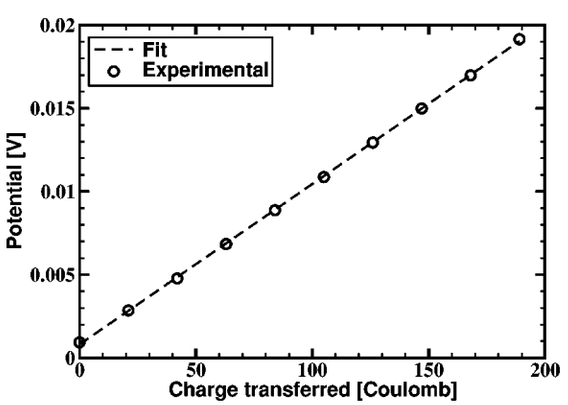

Figure 7. Potential difference at 21°C as a function of charge transferred starting with a 1.74 M $LiPF_6$ electrolyte in both chambers. The electrolyte chambers contained 9.53 and 9.56 mL of electrolyte, respectively.

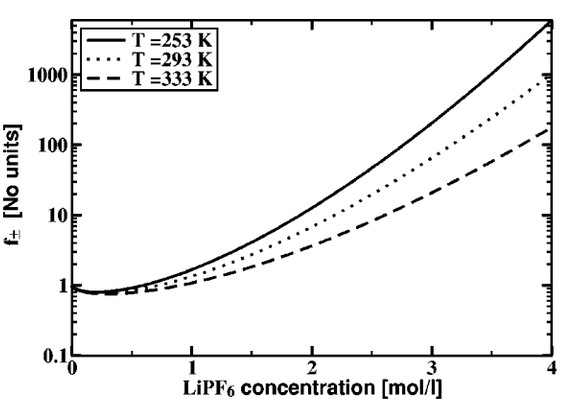

Figure 9. The activity coefficient calculated by integrating $v(c,T)$ from Table I.

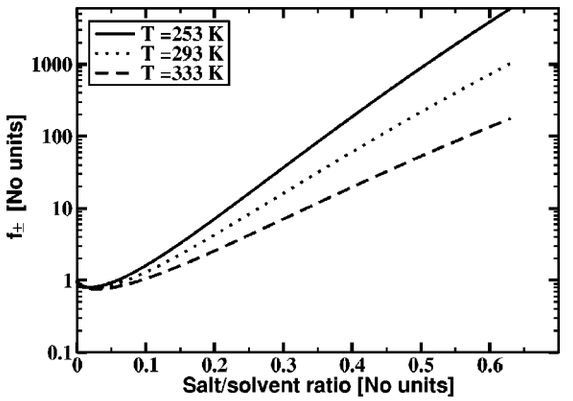

Figure 10. Activity coefficient as a function of $LiPF_6$ salt molecules per solvent molecule.

the activity coefficient is calculated using Eq. 6 and applying the parameters shown in Table I.

The increase in the activity coefficient cannot be explained by ion association, which would have the opposite effect. According to Bockris and Reddy,[25] interactions in electrolytes with no current flowing can be divided into long-range ion-ion coulombic interactions and short-range ion-solvent interactions. The short-range interactions can be ignored for extreme dilution, but they become nonnegligible for medium concentrations ($\sim$0.4 − $\sim$2 M) and have the potential of becoming dominant for high concentrations ($>$ $\sim$2.5 M) in aqueous solutions. Also for aqueous solutions, the activity coefficient is strongly dependent on the hydration number at higher concentrations. For nonaqueous electrolytes, the situation becomes more complicated, but it is evident from the experimental data shown in Fig. 6 and 9 that a similar situation to hydration occurs even at very low concentrations. The best description may be that the solvation shells of the Li^+ and PF_6^- ions are complete only at extreme dilution, and become incomplete even at very low concentrations. This lowers the effective solvent concentration, increasing the driving force (measured potential) for equilibration of two solutions with different concentrations.

To have a closer look at the solvation ratio, the activity coefficient can be graphed as a function of the $LiPF_6$ to solvent ratio, as shown in Fig. 10.

The solvation shell can be estimated to be complete, preventing ion-ion interactions at ratios smaller than approximately salt/solvent =0.01. One can observe that the effective concentration is double that of the real concentration already when salt/solvent =0.1 (−20°C). Moreover, the logarithm of activity *vs.* the salt/solvent ratio exhibits a linear relationship for ratios greater than approximately 0.1. The small deviation downward at high concentrations may be linked to a minor deviation in the fit for $\upsilon(c,T)$ for the highest concentrations, as can be observed from Fig. 5.

Diffusion coefficient.—Galvanostatic polarization.—The method[30] consists of three steps: (*i*) The cell is allowed to rest at open circuit until equilibrated, (*ii*) a small current is applied for a predetermined time during which a concentration gradient builds near each electrode, and (*iii*) the current is switched off and the relaxation of the OCP is monitored. The relaxation is expected to be linear in reduced time

$$\tau = \frac{\sqrt{t}}{\sqrt{t + \sqrt{(t - t_t)}}} \qquad [12]$$

where t is real-time, and t_t is the time when the current was turned off, and relaxation begins. τ can be a bit counterintuitive because $t = t_t$ corresponds to $\tau = 1$, and $t = \infty$ corresponds to $\tau = 0$. In Fig. 11, a typical relaxation curve for 2.24 M $LiPF_6$ in PC/EC/DMC, 21°C, is given.

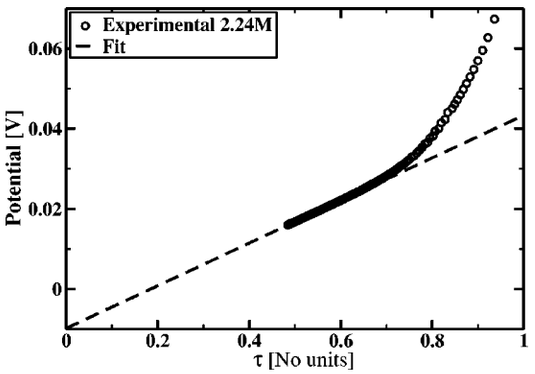

Figure 11. Relaxation curve for 2.24 M $LiPF_6$ in PC/EC/DMC, 21°C.

In the beginning of the relaxation curve (near $\tau = 1$), the rearrangement of the double layer dominates, whereas later on the diffusion dominates and linear behavior ensues. The fit in the diffusion-dominated region was used to determine the extrapolated OCP at $\tau = 1$, in the absence of double-layer effects. Any intercept at $\tau = 0$ was subtracted from the extrapolated OCP at $\tau = 1$ to correct for any experimental voltage offset. Care was taken to select an appropriate current; a too low current would give an insufficient concentration gradient and high experimental error, whereas a too high current would heat the electrolyte and result in erroneous results for the diffusion coefficient.

For a given electrolyte the extrapolated OCV is then determined for numerous values of applied current I or pulse time t_t. It turns out[30] that the OCV(I,t_t) is a linear function of $I\sqrt{t}$, with slope

$$m = \frac{(1 - t_+)4RT\upsilon(c,T)}{F^2 c_o \sqrt{D\pi}} \qquad [13]$$

As usual D cannot be extracted until some other electrolyte properties are known. Fortunately we already have values for t_+ and, $\upsilon(c,T)$.

In Fig. 12 we show some OCV *vs.* $I\sqrt{t}$ graphs for 1.7 M $LiPF_6$ in PC/EC/DMC at various temperatures.

From Fig. 12 it can be seen that a reasonable fit was obtained for all the temperatures. The slope of the lines showed a clear temperature dependence; high slopes for low temperatures and low slopes for high temperatures. It is worthwhile to comment that for several data points, the distance between the data point and the fit line is significant. This can also be observed in the data of Hafezi and Newman.[30] The reason for this deviation is likely complex, but mea-

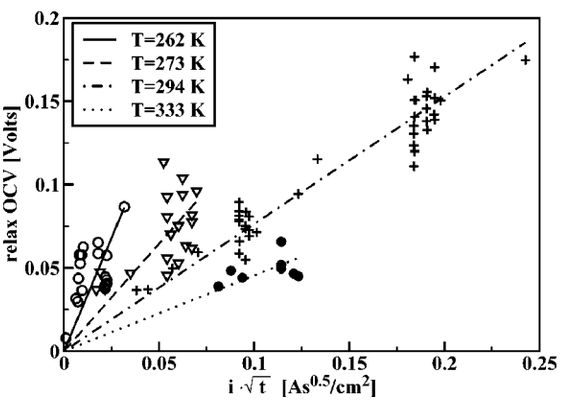

Figure 12. OCPs *vs.* $I\sqrt{t}$ for c = 1.7 M.

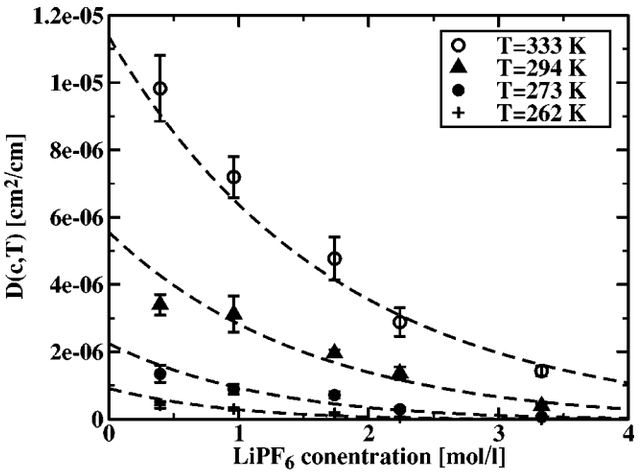

Figure 13. Measured diffusion coefficient as a function of concentration for different temperatures. Error bars represent errors in slope form fitting relaxation data to Eq. 13.

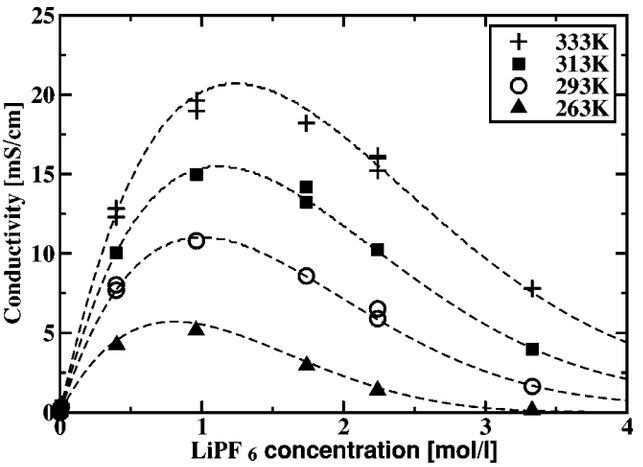

Figure 14. Conductivity of $LiPF_6$ in PC/EC/DMC as a function of $LiPF_6$ concentration for 333, 313, 293, and 263 K.

surements involving the application of a current across a Li metal/$LiPF_6$-containing electrolyte interface are subject to significant experimental variation as the Li electrode activity cannot be considered constant across the Li surface. In the case of Li plating, dendrite formation is known to occur. Another potentially nonquantifiable source of error is electrolyte convection. Electrolyte convection can be caused either by mechanical vibrations or by variations in temperature. Convection can increase the slopes in Fig. 11, thereby decreasing the estimate for the diffusion coefficients, or it could decrease the estimated OCV at $\tau = 1$, resulting in a too high estimate for the diffusion coefficient. By applying a current across a resistive interface, the interface temperature inevitably increases. This temperature increase is dependent on the magnitude of the current and the time this current was applied. Effects from interface heating were observed for some low-temperature measurements, and those results were omitted in the further analysis. To counteract for this heating effect, a low current was applied for an extended amount of time rather than a very high current for a short period of time to obtain an as high as possible number for $I\sqrt{t}$. Under normal conditions, the leak current resulting from the voltage measurements could be ignored as the resistance in the voltmeter was in excess of 1 GΩ, whereas the cell resistances were measured to be in the kΩ range.

As was the case for the activity, it is useful to have an analytic form for $D(c,T)$. One possibility is to expand the diffusion function is a polynomial in log space

$$\ln[D(c)] = D_0(T) + D_1(T) \times c + D_2(T) \times c^2 \ldots \quad [14]$$

where each D_i is expanded as an inverse function of temperature relative to a so-called glass transition temperature T_g which is concentration dependent

$$D_i = D_{i0} + \frac{D_{i1}}{T - T_g(c)} + \frac{D_{i2}}{(T - T_g(c))^2} \cdots \quad [15]$$

where

$$T_g(c) = T_{g0} + cT_{g1} \quad [16]$$

In Fig. 13 the diffusion coefficient as a function of concentration and temperature for −10 to +60°C is given. It can be observed that, as expected, the $LiPF_6$ diffusion coefficient decreases with concentration and increases with temperature.

The magnitudes of the diffusion coefficients are similar to what have been previously reported for EC/EMC[19] and EC/DEC,[32] indicating that the diffusion coefficient is limited in its dependence on the solvent mixture. The error bars in Fig. 13 represent errors in slope form fitting relaxation data to Eq. 13 and do not include possible errors or systematic deviations in the relaxation data. The true error bars are therefore likely somewhat bigger than indicated in Fig. 13. The resulting expansion coefficients giving the dashed lines in Fig. 13 are shown in Table II.

Finally, with the diffusion coefficient calculated, it can be confirmed that the cell length is suitable for the galvanostatic polarization method. According to Ref. 30, the test cell exhibits semi-infinite diffusion as long as $\sqrt{4Dt_i} < L/2$. With the maximum of diffusion coefficients on the order of $1 \times 10^{-5}\mathrm{cm}^2/\mathrm{s}$, the length is suitable for applying current for more than 100 min, whereas for a diffusion coefficient one order of magnitude lower, the cell length is sufficient for applying current up to approximately 17 h. Hafezi and Newman[30] claim that the galvanostatic polarization method is best suited for polymer electrolytes. Electrolytes for Li-ion batteries exhibit properties somewhere between aqueous and polymer electrolytes, having lower specific conductivity, higher viscosity, and lower

Table II. Parameters determining the diffusion coefficient as a function of temperature and concentration.

Parameter	Value	σ	σ(%)	$C_{D_{00}}$	$C_{D_{01}}$	$C_{D_{10}}$	$C_{T_{g_0}}$	$C_{T_{g_1}}$
D_{00}	−4.43	0.06	1.3	100	−84	−2	−66	36
D_{01}	−54	6	10.8	−84	100	−42	94	−71
D_{10}	−0.22	0.02	7.0	−2	−42	100	−55	69
D_{11}	0	0	0	-	-	-	-	-
T_{g_0}	229	3	1.2	−66	94	−55	100	-90
T_{g_1}	5.0	0.5	9.9	36	−71	69	−90	100

Table III. The κ_{ij} coefficients from Eq. 17 found to most truthfully represent the experimental data.

κ_{ij}	j = 0	j = 1	j = 2
i = 0	−10.5	0.0740	-6.96×10^{-5}
i = 1	0.668	−0.0178	2.80×10^{-5}
i = 2	0.494	-8.86×10^{-4}	0

diffusion coefficients than the aqueous electrolytes but still being in a liquid state. We therefore consider this method useful for liquid nonaqueous electrolytes as well.

Conductivity.—Although this is not the focus of this paper, for completeness we include the measured and regressed conductivity for our particular electrolyte recipe. In Fig. 14 the conductivity for $LiPF_6$ in PC/EC/DMC at 263, 293, 313, and 333 K is given.

The continuous lines are least-square fits to Eq. 17, describing the relation between molar conductivity and $LiPF_6$ concentration. Empirically we find the following functional form the most efficient (requires the least number of terms)

$$\sqrt{\frac{\kappa(c,T)}{c}} = \sum_{i=0}^{n}\sum_{j=0}^{k} \kappa_{ij} c^i T^j \qquad [17]$$

The κ_{ij} coefficients found to most truthfully represent the experimental data are given in Table III.

Voltage Profile in a Real Cell

The value of our measured transport (and thermodynamic) properties rests with their predictive power. In principle we should now be able to accurately reproduce the voltage profile and self-heating effects of a known cell design running at a high current. Techniques for these calculations are now well established,[10,12,34-36] the details of which are well outside the scope of this work. In order to perform these calculations we developed our own software which differs from previous implementations[34-36] in a number of ways, which will be described in a future publication.

In addition to testing predictions based on our measured electrolyte properties by comparing with measured cell data, it is also of interest to compare with predictions based on partial (little or no *c*, *T* dependence) electrolyte properties that have been used previously in the literature for such calculations. In addition we show results for a intermediate situation with ideal activity and constant/averaged salt diffusion.

Figure 15 shows simulated voltage curves for a 65 mm high × 26 mm diam cylindrical Li-ion battery with graphite and spinel ($LiMn_2O_4$) electrodes. The externally applied current, starting temperature, and concentration are 5 A (1.7 C), 25°C, and 0.96 M, respectively. The relatively low current of 5 A was selected because the cathode concentration by the foil just reached zero by the end of the discharge using this current. The skin temperature of the energy-optimized cell was measured to be 40°C at the end of the discharge, almost doubling the $LiPF_6$ diffusion coefficient for 0.96 M compared to the starting temperature.

From Fig. 15 one can observe that by applying the transport properties as measured in the present paper, the cell voltage during a discharge can be calculated to a rather high degree of accuracy. In the figure, other voltage curves incorporating various other representations of the transport properties are also shown. The activity coefficient relates the voltage drop resulting from a concentration gradient. In light of the high activity coefficients measured and shown in Fig. 9, it can be expected that using $f_\pm = 1$ would give an insufficiently small voltage drop for a given concentration gradient compared to a real cell. This is exactly what can be observed from Fig. 15. This partially explains why previous workers commonly had to invoke a rather large so-called film and/or contact resistance in the calculation. We found no need for any such resistance parameters. It is, however, worthwhile to mention that a film/and or contact resistance would be highly correlated to the exchange current density for a constant current discharge. From the simulations forming the background for Fig. 15, it is clear that failure to take the activity into account has the potential of overstating the importance of any SEI film resistance.

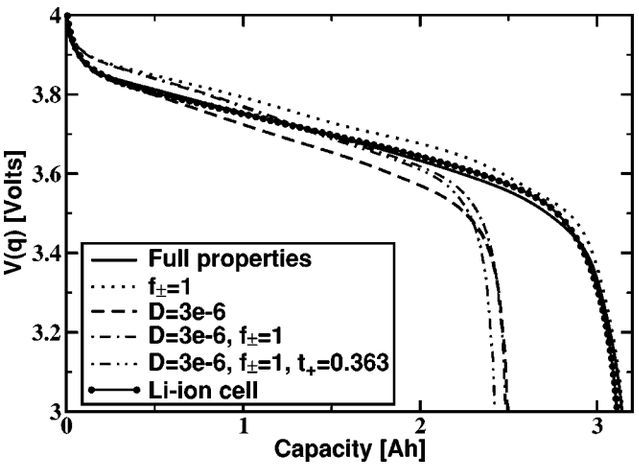

Figure 15. Predicted voltage curves using electrolyte options for the electrolyte properties. Full properties refer to parameters measured and presented in the present paper.

Suppressing the concentration and temperature dependence in the diffusion coefficient is seen to result in a significant voltage drop at the end of the discharge, because self heating can no longer help relax the liquid phase concentration gradients. In particular, see the calculated voltage curve using $f_\pm = 1$ as measured here and a constant diffusion coefficient. Using both $f_\pm = 1$ and a fixed diffusion coefficient incorporates both the effects described, whereas adapting the lower transference number of 0.363 commonly used in the literature is similar to the simulation using the transference number determined in the present paper except for a slightly lower capacity. In summary, Fig. 15 illustrates clearly that in order to have a truthful representation of the discharge voltage, all the electrolyte transport and thermodynamic properties need to be correctly determined as a function of concentration and temperature.

As has been pointed out in the previous literature, an important feature of these calculations is that they allow one to peek inside the electrode stack and view various potentials, currents, and concentration gradients while the cell is under load. This is both a great educational tool as well as allowing a cell design engineer to understand the impact that various mesoscopic processes have on cell voltage suppression and self-heating. In Fig. 16, the $LiPF_6$ concentration profile across the electrode stack after 2.0 Ah is discharged from the cell shown in Fig. 15 using the parameters derived in the present paper. The same parameters for the simulation as used to obtain the results shown in Fig. 15 were applied.

From Fig. 16, it can be observed that changing the transference number from 0.38 to 0.363 or changing the $LiPF_6$ activity to resemble $f_\pm = 1$ for all concentrations a has minor effect on the predicted concentration gradient. Using a diffusion coefficient with a temperature and concentration dependence results in a notably smaller predicted concentration gradient than using a fixed diffusion coefficient with a value close to the starting concentration and temperature of the electrolyte. The reason for this is that as the cell temperature increases during discharge of the cell, the diffusion coefficient increases, resulting in smaller concentration differences across the cell stack. Combining the concentrations from Fig. 16 with the measured diffusion coefficients shown in Fig. 13, there is at least a factor of four difference between the salt diffusion coefficient

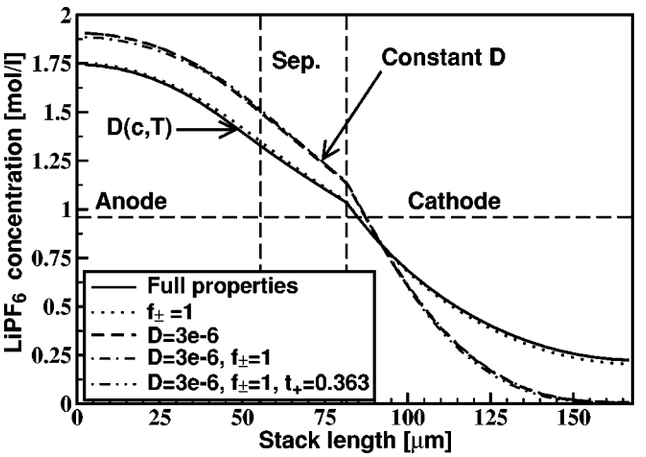

Figure 16. $LiPF_6$ concentration profile across the electrode stack from Fig. 15 after 2.0 Ah had been discharged from the cells.

close to the foil in the anode and the cathode, assuming an average cell temperature of around 35°C after a discharge of 2.0 Ah from the cell.

Conclusion

In order to get a complete picture of the transport processes in an electrolyte intended for utilization in Li-ion batteries, the transference number, diffusion coefficient, as well as the mean $LiPF_6$ activity coefficient all need to be determined as a function of concentration and temperature. The activity coefficients for $LiPF_6$ in PC/EC/DMC were determined to be larger than one for most of the applicable concentration range, indicating solvent immobilization. The transference number showed little variation with concentration and temperature. The diffusion coefficient for our electrolyte was strongly dependent on concentration and temperature. The salt activity was also strongly concentration dependent, but only weakly dependent on temperature at low concentrations. The electrolyte recipe studied here was observed to behave as a concentrated solution even at very low concentrations, 0.1 M. This predicts that any attempt to use dilute or ideal solution theories to understand liquid Li-ion electrolyte is likely to fail.

In order to predict cell voltage under load for a real Li-ion battery, full knowledge of the electrolyte properties is essential. Conversely, this means that electrolyte optimization is an essential component of cell optimization. It also follows that optimizing electrolyte conductivity by itself does not constitute cell optimization, in fact, we believe that conductivity optimization by itself is often deceptive. One might argue that at low currents concentration gradients and self-heating is less important. To some extent this is true, but one must also keep in mind that modern commercial Li-ion cells are optimized for maximum capacity, which translates into minimal pore space in the electrodes. As a result the effective diffusion coefficient is greatly reduced, sometimes by more than an order of magnitude.

We hope that in the future, people doing voltage and self-heating calculations will find these measured electrolyte properties useful for their calculations. It is for this reason we have provided analytic expressions (usually 2 variable polynomials) for all the transport and thermodynamic properties. Modifications in the electrolyte recipe invarably arise, *i.e.*, not everyone is interested our precise recipe. We expect that the properties here will be reasonably valid when minor modifications in the solvent are considered, particularly if the viscosity (and dielectric constant) remains largely unchanged. As more liquid electrolyte systems become fully characterized we expect to learn some rules of thumb that can be applied in such cases. By far the most time-consuming quantity to measure accurately is the diffusion coefficient. Any future work aimed at streamlining this process would be useful.

Acknowledgments

We thank Gavan Eddy for making the electrolytes, and David Jarvis, Jim Chamorsta, and Magdalena Mazur for assisting in performing various measurements. The authors also thank NSERC for financial support. Karen Thomas-Alyea and Sarah Stewart are acknowledged for critical reading of the manuscript and interesting discussions.

E-One Moli Energy (Canada), Limited, assisted in meeting the publication costs of this article.

Appendix

Voltage Profile Calculation Details

Voltage curves were fit with the following empirical function

$$V(x) = V_o + \sum_{i=0}^{n} \frac{A_i}{1 + e^{\beta_i(x-x_i)}} \qquad [A\text{–}1]$$

which is just a constant plus a series of Fermi step-like functions. The fit parameters used in the present paper are given in Table A-I.

To properly model the cell performance, we also need the exchange current density, $i_\circ$, and the entropy $d\Phi/dT$. Anode $d\Phi/dT$ parameters were from Ref. 37, whereas cathode parameters were taken from from Ref. 38. The exchange current densities were found using least squares fitting to experimental data. Values of 0.26 and 0.96 mA/cm^2 were used for the anode and cathode active material, respectively.

Heat capacity (0.8J/gK) and surface emissivity (1.3J/K cm^2) were taken from Hatchard *et al.*[39]

In Table A-II, the cell design used for the voltage simulations are shown. The cell consists of a Cu current collector, on which the anode (negative Li_xC_6 electrode) material is pasted and an Al current collector on which is pasted the cathode (positive $Li_yMn_2O_4$ electrode) material (see Ref. 41 for a detailed cell description). When the cell parameters are known, the performance of a real battery cell can be modeled using well-established techniques.[10,34]

Table A-I. Voltage curve fit parameters according to Eq. 18 for the cathode (positive $Li_yMn_2O_4$ electrode) and anode (negative Li_xC_6 electrode). The parameter V_o was 0.6185 and 0.005769 for the cathode and anode, respectively.

i	A_{ic}	β_{ic}	χ_{0c}	A_{ia}	β_{ia}	χ_{0a}
1	111.1	526.9	−0.003787	53.03	116.4	−0.015616
2	0.8014	27.84	−0.07037	0.3863	57.80	0.05939
3	0.2002	7.841	0.4807	0.7979	31.91	0.2025
4	0.1505	14.60	0.9493	0.03996	21.76	0.5146
5	0.3580	213.1	0.9965	0.04007	19.17	0.8803
6	0.4480	426.3	1.005	0.1534	39.54	1.008
7	0.1941	1133	1.010	−0.1045	36.25	1.026
8	1.176	28.96	1.211	-	-	-
9	1.013	56.22	1.297	-	-	-

Table A-II. Electrode and separator parameters. Separator tortuosity (Bruggeman exponent) and porosity are taken from Patel *et al.*[40]

Quantity	Unit	Anode	Cathode	Separator
Total thickness	mm	0.198	0.185	0.026
Foil thickness	mm	0.015	0.02	N/A
Porosity	%	26.2	26.7	37
Tortuosity	-	2.9	2.8	2.8

List of Symbols

A	Debye-Hückel coefficient, $\sqrt{1/\text{mol}}$
A_i	fit parameter for voltage curve, V
C_{ij}	correlation coefficient
c	concentration, mol/L
c_o	bulk concentration, mol/L
D	diffusion coefficient, cm^2/s
D_{ij}	$D(c,T)$ polynomial expansion coefficient
F	Faraday's constant, 96,487 C/mol
$f_\pm$	mean molar salt activity coefficient
I	current, A
i	current density, A/m^2
i_o	exchange current density, A/m^2
L	cell length
m	slope of OCV, $\text{Vm}^2/\text{A}\sqrt{\text{s}}$
n	moles
R	gas constant, J/molK
T	temperature
T_g	glass transition temperature
t	time, s
t_t	time when current was turned off
t_+	transference number for positive species
V_o	fit parameter for voltage curve, V
v_{ij}	$v(c,T)$ polynomial expansion coefficient
z_i	charge number of species i

Greek

β	fit parameter for voltage curve
Δ	difference
κ	conductivity, mS/cm
κ_{ij}	$\kappa(c,T)$ polynomial expansion coefficient
σ	standard deviation
$\sigma[\%]$	relative standard deviation
τ	dimensionless time
Φ	potential, V
χ_i	fit parameter for voltage curve, V

Subscripts

$+$	positive ion (Li^+)
$-$	negative ion (PF_6^-)
L	left
R	right
a	anode
c	cathode

References

1. A. Wilson and J. Reimers, *J. Power Sources*, **81-82**, 642 (1999).
2. H. J. Gores and J. Barthel, *J. Solution Chem.*, **9**, 939 (1980).
3. M. C. Smart, B. V. Ratnakumar, and S. Surampudi, *J. Electrochem. Soc.*, **146**, 486 (1999).
4. M. Videa, W. Xu, B. Geil, R. Marzke, and C. A. Angell, *J. Electrochem. Soc.*, **148**, A1352 (2001).
5. M. Riley, P. S. Fedkiw, and S. A. Khan, *J. Electrochem. Soc.*, **149**, A667 (2002).
6. J. Barthel, R. Buestrich, E. Carl, and H. J. Gores, *J. Electrochem. Soc.*, **143**, 3565 (1996).
7. S. S. Zhang and C. A. Angell, *J. Electrochem. Soc.*, **143**, 4047 (1996).
8. M. S. Ding, K. Xu, S. S. Zhang, A. Amine, G. L. Henriksen, and T. R. Jow, *J. Electrochem. Soc.*, **148**, A1196 (2001).
9. H. P. Chen, J. W. Fergus, and B. Z. Jang, *J. Electrochem. Soc.*, **147**, 399 (2000).
10. M. Doyle, J. Newman, A. S. Gozdz, C. N. Shmutz, and J. M. Tarascon, *J. Electrochem. Soc.*, **143**, 1890 (1996).
11. J. Newman, *Electrochemical Systems*, 2nd ed., Prentice Hall, Englewood Cliffs, NJ (1991).
12. K. E. Thomas, R. M. Darling, and J. Newman, in *Advances in Lithium-Ion Batteries*, W. van Schalkwijk and B. Scrosati, Editors, pp. 342-392, Kluwer Academic/Plenum Publishers, New York (2002).
13. J. Newman, K. Thomas, H. Hafezi, and D. Wheeler, *J. Power Sources*, **119-121**, 838 (2003).
14. M. Doyle and Y. Fuentes, *J. Electrochem. Soc.*, **150**, A706 (2003).
15. J. M. Sullivan, D. C. Hanson, and R. Keller, *J. Electrochem. Soc.*, **117**, 779 (1970).
16. D. Jasinski, *Advances in Electrochemistry and Electrochemical Engineering*, Vol. 8, John Wiley & Sons, New York (1972).
17. K. West, T. Jacobsen, and S. Altung, *J. Electrochem. Soc.*, **129**, 1480 (1982).
18. M. W. Verbugge, *AIChE J.*, **41**, 1550 (1995).
19. C. Capiglia, Y. Saito, H. Kageyama, P. Mustarelli, T. Iwamoto, T. Tabuchi, and H. Tukamoto, *J. Power Sources*, **81-82**, 859 (1999).
20. P. Georen and G. Lindbergh, *Electrochim. Acta*, **49**, 3497 (2004).
21. Y. Ma, M. Doyle, T. F. Fuller, M. M. Doeff, L. C. De Jonghe, and J. Newman, *J. Electrochem. Soc.*, **142**, 1859 (1995).
22. A. Ferry, M. M. Doeff, and L. C. De Jonghe, *Electrochim. Acta*, **43**, 1387 (1998).
23. M. M. Doeff, L. Edman, S. E. Sloop, J. Kerr, and L. C. De Jonghe, *J. Power Sources*, **89**, 227 (2000).
24. J. Newman and K. Thomas-Alyea, *Electrochemical Systems*, 3rd ed., John Wiley & Sons, Inc., Hoboken, NJ (2004).
25. J. Bockris and A. Reddy, *Modern Electrochemistry*, Vol. 1, 2nd ed., Plenum Press, New York (1998).
26. K. Laidler and J. Meiser, *Physical Chemistry*, Benjamin/Cummings Publishing Company, Menlo Park, CA (1982).
27. M. Clericuzio, W. Parker Jr., M. Soprani, and M. Andrei, *Solid State Ionics*, **82**, 179 (1995).
28. Y. Aihara, T. Bando, H. Nakagawa, H. Yoshida, K. Hayamizu, E. Akiba, and W. Price, *J. Electrochem. Soc.*, **151**, A119 (2004).
29. K. Gering and T. Duong, in *Lithium/Lithium Ion Batteries*, K. Striebel, Editor, The Electrochemical Society Proceedings Series, Pennington, NJ (2003), In press.
30. H. Hafezi and J. Newman, *J. Electrochem. Soc.*, **147**, 3036 (2000).
31. J. Newman and T. Chapman, *AIChE J.*, **19**, 343 (1973).
32. C. Capiglia, H. Saito, Y. Yamamoto, H. Kageyama, and P. Mustarelli, *Electrochim. Acta*, **45**, 1341 (2000).
33. D. Pletcher, *A First Course in Electrode Processes*, The Electrochemical Consultancy, England (1991).
34. T. Fuller, M. Doyle, and J. Newman, *J. Electrochem. Soc.*, **141**, 1 (1994).
35. M. Doyle, T. Fuller, and J. Newman, *J. Electrochem. Soc.*, **140**, 1526 (1993).
36. T. Fuller, M. Doyle, and J. Newman, *J. Electrochem. Soc.*, **141**, 982 (1994).
37. K. Thomas and J. Newman, *J. Power Sources*, **119-121**, 844 (2003).
38. Y.-S. Lin and J. Reimers, Extended Abstracts. The 12th International Meeting on Lithium Batteries, Nara, Japan (2004).
39. T. Hatchard, D. MacNeil, A. Basu, and J. Dahn, *J. Electrochem. Soc.*, **148**, A755 (2001).
40. K. Patel, J. Paulsen, and J. Desilvestro, *J. Power Sources*, **122**, 144 (2003).
41. P. Arora, M. Doyle, and R. White, *J. Electrochem. Soc.*, **146**, 3543 (1999).